

# High-precision measurement of hyperfine structure in the $D$ lines of alkali atoms

Dipankar Das and Vasant Natarajan

Department of Physics, Indian Institute of Science, Bangalore 560 012, INDIA

E-mail: [vasant@physics.iisc.ernet.in](mailto:vasant@physics.iisc.ernet.in)

**Abstract.** We have measured hyperfine structure in the first-excited  $P$  state ( $D$  lines) of all the naturally-occurring alkali atoms. We use high-resolution laser spectroscopy to resolve hyperfine transitions, and measure intervals by locking the frequency shift produced by an acousto-optic modulator to the difference between two transitions. In most cases, the hyperfine coupling constants derived from our measurements improve previous values significantly.

PACS numbers: 32.10.Fn,39.30.+w,42.62.Fi

## 1. Introduction

High-precision measurement of hyperfine structure in the excited states of alkali atoms provides a stringent testing ground for state-of-the-art atomic calculations based on the best wavefunctions [1], because it is sensitive to effects such as core polarization and electron correlation. The  $D_2$  line of alkali atoms is routinely used in laser cooling and Bose-Einstein condensation experiments. These ultracold atoms are important in experiments ranging from fundamental physics issues such as high-resolution spectroscopy, measurement of fundamental constants, and the study of cold collisions, to applications in atomic clocks and inertial sensors. Heavy alkali atoms are also important in studies of atomic parity violation and the search for a permanent atomic electric dipole moment. In these experiments, accurate calculations are needed to properly interpret the experimental results. In addition, hyperfine structure provides important information about the structure of the nucleus, i.e. the multipole moments of its charge and current distribution [2].

Hyperfine structure has been measured with high accuracy in the ground state of alkali atoms using atomic beam magnetic resonance techniques. Thus the hyperfine constants are known with a relative precision of better than  $10^{-9}$ . Indeed, this high precision of the measurements has led to the definition of the SI unit of time in terms of the ground hyperfine interval in Cs. However, measurement of hyperfine structure in the excited state is often limited by the linewidth of the transition, which is about 5–10 MHz for the  $D$  lines of alkali atoms. The advent of narrow linewidth tunable lasers (ring dye lasers and frequency-stabilized diode lasers) and high-resolution Doppler-free spectroscopy techniques (such as saturated-absorption spectroscopy) has allowed individual hyperfine transitions to be resolved. But there is still an issue of frequency calibration and linearity of the laser scan axis. We have solved this problem by using an acousto-optic modulator (AOM), driven by a easily-measured radio frequency source, to span the difference between hyperfine transitions. We are thus able to measure hyperfine intervals in the  $D$  lines of alkali atoms with a typical precision of 1–2 parts in 1000 of the linewidth. In earlier work, we had reported measurement of hyperfine structure in a few alkali atoms. In the current work, we present comprehensive results on all the naturally-occurring alkali atoms. The results, in most cases, are consistent with previously published values but represent a significant improvement in precision.

Let us first consider the definition of the hyperfine constants. The basis states used for defining hyperfine structure are the  $|J, I, F, m_F\rangle$  states, where  $J$ ,  $I$ , and  $F$  are the quantum numbers associated with, respectively, the electronic angular momentum  $\mathbf{J}$ , the nuclear spin  $\mathbf{I}$ , and the total angular momentum  $\mathbf{F} = \mathbf{I} + \mathbf{J}$ . In the approximation that  $J$  and  $I$  are good quantum numbers, the hyperfine interaction energy  $W_F$  is given by,

$$W_F = \frac{1}{2}hAK + hB \frac{\frac{3}{2}K(K+1) - 2I(I+1)J(J+1)}{2I(2I-1)2J(2J-1)},$$

where  $K = F(F+1) - I(I+1) - J(J+1)$ ,  $A$  is the magnetic-dipole coupling constant,

and  $B$  is the electric-quadrupole coupling constant.

The first excited  $P$  state of alkali atoms splits into two states,  $P_{1/2}$  and  $P_{3/2}$ , due to spin-orbit interaction (fine-structure splitting). Of these, the  $P_{1/2}$  state ( $D_1$  line) further splits into two hyperfine levels with energy shifts determined by the magnetic-dipole interaction. The electric-quadrupole interaction is present only for  $I, J \geq 1$ , and hence does not affect this state. On the other hand, the  $P_{3/2}$  state ( $D_2$  line) splits into four hyperfine levels with energy shifts determined by both interactions. In the case of  $^{133}\text{Cs}$ , we will see later that there is evidence of a small additional contribution from a magnetic-octupole hyperfine interaction.

## 2. Experimental technique

The experimental schematic to measure hyperfine intervals is shown in Fig. 1, and is essentially the same for all atoms. The output from a frequency-stabilized tunable laser is split into two parts. The first part goes into an atomic spectrometer, the signal from which is used to lock the laser to a particular hyperfine transition. The second part is frequency shifted through an AOM and then sent into a second atomic spectrometer. The frequency of the AOM is adjusted so that the shifted beam is on a neighboring hyperfine transition. The error signal from this peak is fed back to the AOM driver to lock its frequency. Thus the AOM frequency gives a direct measurement of the hyperfine interval. For intervals that are too small or too large to be measured with a single AOM, we use an additional AOM with a fixed frequency offset.

The  $D$  lines in sodium are in the visible (at 589 nm), hence the tunable laser is a ring dye laser (Coherent 699-21). The laser is frequency stabilized to a reference cavity that gives it an instantaneous linewidth of 1 MHz. The  $D$  lines in all the other atoms are in the near infrared which can be accessed using diode lasers. The diode laser is frequency stabilized using optical feedback from a piezo-mounted grating so that the resulting linewidth is about 500 kHz. The linewidth is reduced considerably when the laser is locked. For locking, the laser is frequency modulated at  $f = 20$  kHz, and the signal from the spectrometers is demodulated at  $3f$  to generate the error signals. Such third-harmonic detection provides narrow dispersive signals that are insensitive to intensity fluctuations, to peak pulling from neighboring transitions, or to any residual Doppler profile in the spectrum [3].

In the case of Li, the spectroscopy is done using a collimated atomic beam. The atoms are excited by a perpendicular laser beam, and the resulting Doppler-free fluorescence signal is measured with a photomultiplier tube (PMT). In all the other atoms, we use absorption spectroscopy of a probe beam through a vapor cell. The cell is either at room temperature (Rb and Cs) or heated to 75°C (Na and K), to have an atomic density of about  $10^9$  cm $^{-3}$ . In order to get Doppler-free absorption spectra, we use one of two techniques. The first technique is the normal saturated-absorption spectroscopy (SAS) [4], where a strong counter-propagating pump beam decreases the absorption of the weak probe beam on resonance. As is well known, the SAS technique

produces additional crossover resonances, which occur exactly midway between two hyperfine peaks. For closely-spaced levels, the large crossover resonances often swamp the true peaks. This is a problem especially in the  $D_2$  lines of Na and K, where the level spacing is of the order of one or two natural linewidths.

To overcome this problem, we have recently developed an alternate technique of high-resolution spectroscopy, which we call coherent-control spectroscopy (CCS) [5, 6, 7]. This technique uses co-propagating control and probe beams, and does not produce crossover resonances. The probe beam is locked on to a hyperfine transition, while the control beam is scanned across a neighboring transition. When the control comes into resonance with a transition coupling to the same ground level, it “coherently” reduces probe absorption through a process similar to electromagnetically induced transparency. Since the probe is locked on a transition, it addresses only the zero-velocity atoms, and the resultant lineshape remains Doppler-free even in hot vapor.

We have also done a density-matrix analysis of the effective three-level atom in the presence of the probe and control beams. The calculated lineshape, after accounting for thermal averaging in hot vapor, describes the measured spectrum quite well [6]. Apart from the ability to resolve closely-spaced levels, another important advantage of the CCS technique for measuring hyperfine intervals is that the measured value is completely insensitive to detuning of the probe beam. Any detuning of the probe from resonance would imply that it is resonant with a non-zero velocity group. Since the control beam co-propagates with the probe beam, the spectrum will show peaks only when the control beam comes into resonance with the same non-zero velocity group, which happens only when the AOM shift matches the hyperfine interval. Thus, as the probe beam is detuned from resonance, the manifold of peaks (corresponding to the different hyperfine levels) will shift within the Doppler profile, but their relative separation will remain the same.

### 3. Error Analysis

The different sources of error in the measurement have been discussed extensively in our earlier publications, and are reviewed here for completeness.

#### 3.1. Statistical errors

The primary sources of statistical error are the fluctuations in the lock point of the laser and the AOM. To minimize these errors, we use an integration time of 10 s in the frequency counter during each measurement of the AOM frequency. Then we take an average of 35–40 measurements for a given transition, and repeat the set several times. The resulting standard deviation (scatter) in the data set is about 10 kHz, from which we take the statistical error in the mean to be  $\sim 2$  kHz. The timebase in the frequency counter used for measuring the AOM frequency has a stability of better than  $10^{-6}$ , which translates to a negligible error of  $< 0.1$  kHz in the frequency measurement.

### 3.2. Systematic errors

Systematic errors can occur if there are systematic shifts in the lock points of the laser and the AOM. This can arise due to one of the following reasons.

- (i) *Radiation-pressure effects.* Radiation pressure causes velocity redistribution of the atoms in the vapor cell. In the SAS technique, the opposite Doppler shifts for the counter-propagating beams can result in asymmetry of the observed lineshape [8]. We minimize these effects by using beam intensities that are much smaller than the saturation intensity. In the CCS technique, radiation pressure effects are less important because the Doppler shift will be the same for both beams and will not affect the hyperfine interval, similar to how the interval is insensitive to any detuning of the probe from resonance.
- (ii) *Effect of stray magnetic fields.* The primary effect of a magnetic field is to split the Zeeman sublevels and broaden the line without affecting the line center. However, line shifts can occur if there is asymmetric optical pumping into Zeeman sublevels. For a transition  $|F, m_F\rangle \rightarrow |F', m_{F'}\rangle$ , the systematic shift of the line center is  $\mu_B(g_{F'}m_{F'} - g_F m_F)B$ , where  $\mu_B = 1.4 \text{ MHz/G}$  is the Bohr magneton,  $g$ 's denote the Landé  $g$  factors of the two levels, and  $B$  is the magnetic field. The selection rule for dipole transitions is  $\Delta m = 0, \pm 1$ , depending on the direction of the magnetic field and the polarization of the light. Thus, if the beams are linearly polarized, there will be no asymmetric driving and the line center will not be shifted. We therefore minimize this error in two ways. First, we use polarizing cubes to ensure that the beams have near-perfect linear polarization. Second, we use a special magnetic shield [9] around the cells to minimize the field. The residual field (measured with a 3-axis fluxgate magnetometer) is below 5 mG with one layer of shielding, and further reduces to 1 mG with two layers.
- (iii) *Phase shifts in the feedback loop.* We check for this error by replacing the AOM with two identical AOMs, and adjusting them so that they produce opposite frequency offsets. With the laser locked to a given hyperfine transition, the first AOM then produces a fixed frequency offset which is compensated by the second AOM. Thus the same hyperfine transition is used for locking in both spectrometers. Under these conditions, the second AOM should lock to the fixed frequency of the first AOM, with any error arising solely due to phase-shift errors. We find that the second AOM tracks the frequency of the first AOM to within 1 kHz.
- (iv) *Shifts due to collisions.* To first order, collisional shifts are the same for different hyperfine levels, and hence do not affect the interval. Small differential shifts of the interval have been studied carefully in the ground state of Cs, due to its importance in atomic clocks. However, the size of the shift is in the mHz range [10]. We have also studied shifts in the excited state of Cs by repeating the measurements with a heated vapour cell. An increase from 25°C to 45°C increases the Cs density by a factor of 5, and we find that the measured values shift by less than 5 kHz. We therefore estimate that the maximum shift due to collisions is 5 kHz.

The sizes of the various sources of error are listed in Table 1. The size of the Zeeman shift is calculated in each atom by considering all allowed combinations of  $m_F$  and  $m_{F'}$  and taking the one with the largest shift, assuming atoms get completely optically pumped into these sublevels.

As mentioned in point (i) above, the peak center can be shifted due to radiation-pressure effects. Similarly, from point (ii), the center can be shifted if there is *asymmetric* pumping into the Zeeman sublevels in the presence of a residual magnetic field. Asymmetric optical pumping can occur if the beam polarizations are not perfectly linear, for example due to imperfections in the cubes or birefringence at the cell windows. Finally, there can be a small AC Stark shift of the transition due to nearby hyperfine levels from which the laser is detuned. From an experimental point of view, all these effects will change with laser power. Therefore, we can check for these errors by repeating the measurements at different values of power, and extrapolate to zero power if necessary.

#### 4. Lithium

We now consider the hyperfine measurements in each atom in turn. We present a detailed description of the measurement in Li for several reasons. First, Li is the only atom in which we use an atomic beam for spectroscopy. Therefore, it is slightly different from the vapor-cell technique used in other atoms, which has been described in detail in our earlier publications. Second, we give a complete list of the hyperfine intervals measured at different powers. As mentioned above, this method is used to check for intensity-dependent errors, and we just present a summary of the results in the other atoms. Finally, the small ground hyperfine interval in Li offers a unique possibility of checking the reliability of our technique, which is not easy in the other atoms.

Lithium has two stable isotopes:  ${}^6\text{Li}$  with  $I = 1$  and natural abundance of 7.3%, and  ${}^7\text{Li}$  with  $I = 3/2$  and natural abundance of 92.7%. Li spectroscopy was done using a collimated atomic beam generated by heating a stainless steel oven containing Li metal to 300°C. The oven was placed inside a vacuum chamber maintained at a pressure below  $5 \times 10^{-8}$  torr with a 20 l/s ion pump. The atomic beam was excited with a perpendicular laser beam generated from a home-built diode laser system operating at 670 nm. The laser beam was linearly polarized and the interaction region was shielded with a two-layer magnetic shield. The resulting Doppler-free fluorescence signal was detected by a PMT (Hamamatsu R928).

We obtained spectra from the  $D$  lines of both isotopes. In the  $D_1$  line, the individual hyperfine transitions are well resolved and we can lock to each peak separately. However, in the  $D_2$  line, the different transitions are only partially resolved because the level spacing is less than the natural linewidth. In recent work where we measured the absolute frequencies of these transitions [11], we showed that a multiplex fit to the partially-resolved spectrum yields the hyperfine constants in the  $2P_{3/2}$  state with a precision of about 50 kHz. This is less than the precision with which they are known from earlier experiments. Therefore, in this work we report hyperfine structure only in

the  $2P_{1/2}$  state.

#### 4.1. $D_1$ line

Typical spectra for the  $D_1$  line in the two isotopes of Li are shown in Figs. 2(a) and (b). The four hyperfine transitions in each isotope are clearly resolved. Close-up scans (normalized) of a representative peak in each isotope are shown in Figs. 2(c) and (d), respectively. The solid lines are Lorentzian fits showing the excellent fit with featureless residuals. The size of the residuals gives an idea of the overall signal to noise ratio. The fit linewidth is  $9.0 \pm 0.25$  MHz (compared to the natural linewidth of 5.87 MHz), indicating that the atomic beam is well collimated because the spread in transverse velocity increases the total linewidth by only about 50%. The laser linewidth does not contribute significantly to this broadening.

An important consideration in atomic beam experiments is the systematic Doppler shift of line center that can occur if the laser beam is not perfectly orthogonal. In the recent work on absolute frequency measurements of the  $D$  lines [11], we used the same spectrometer to measure the frequencies with laser beams traversing the atomic beam in opposite directions. Since the Doppler shift is opposite for the two cases, their difference gives a measure of the misalignment from perpendicularity. Our measurements show that the Doppler shift of the transition frequency is only 150 kHz, corresponding to a misalignment angle of 0.1 mrad. For the hyperfine interval, this implies a negligible error of less than 1 Hz.

In order to measure the hyperfine intervals, both the unshifted laser beam and the AOM-shifted beam were sent across the atomic beam. The diode laser and the AOM were modulated at different frequencies, and the signal from the PMT was independently demodulated at the two frequencies. The first error signal was used to lock the laser on a given hyperfine transition, while the second error signal was used to lock the AOM to the hyperfine interval.

A stringent check on our error estimate in Table 1 is to use our technique to measure the ground hyperfine interval. As mentioned in the Introduction, this interval is already known in all alkali atoms with  $< 10^{-9}$  relative precision. However, our technique requires the interval to be accessible with an AOM, and this is possible only in  ${}^6,{}^7\text{Li}$ , where the intervals are about 200 MHz and 800 MHz respectively. Among the different sources of error in this measurement considered before, the effect of collisions is negligible in an atomic beam. We can also check for the intensity-dependent errors by varying the laser power. The results of ground hyperfine measurements at three powers are shown in Table 2. The beam size is such that the peak intensity (at beam center) for the highest power of  $42 \mu\text{W}$  is  $0.84 \text{ mW/cm}^2$ , which is still smaller than the saturation intensity of  $2.51 \text{ mW/cm}^2$ .

The important thing to note from the table is that all the measurements lie within a few kHz of each other, even when the laser power is increased by a factor of three. This means that shifts due to radiation-pressure and optical-pumping effects are less

than 5 kHz, consistent with our earlier estimate. Note that increasing the laser power also increases the height of the peaks in the spectrum, their linewidth, and the overall signal-to-noise ratio. The consistency of the values shows that there are no unknown systematic errors related to these parameters. To see if there is any intensity-dependent trend in the data, we have plotted the measured values versus power in Fig. 3. The linear fit has a small slope, and the extrapolated values of the intervals are

$${}^6\text{Li}, 2S_{1/2}: \Delta\nu_{\frac{3}{2}-\frac{1}{2}} = 228.205(6) \text{ MHz.}$$

$${}^7\text{Li}, 2S_{1/2}: \Delta\nu_{2-1} = 803.504(6) \text{ MHz.}$$

The quoted error of 6 kHz is the total error obtained by adding in quadrature the different sources of error in Table 1. All the values in the table lie within 6 kHz of the extrapolated value for  ${}^6\text{Li}$ , and 10 kHz for  ${}^7\text{Li}$ . These values can be compared with the accurately known values [2]: 228.205 261 1 MHz in  ${}^6\text{Li}$  and 803.504 086 6 MHz in  ${}^7\text{Li}$ . Our values are consistent within  $1\sigma$ , confirming that our error estimate is reasonable.

We now turn to the measurement of hyperfine intervals in the  $2P_{1/2}$  state. Since there are two ground hyperfine levels, the same interval can be measured with transitions starting from either level. As before, the measurements were done at three laser powers as listed in Table 2. The measurements at the different powers again lie within a few kHz of each other. The measurements are plotted against power to yield extrapolated values of the intervals as

$${}^6\text{Li}, 2P_{1/2}: \Delta\nu_{\frac{3}{2}-\frac{1}{2}} = \frac{3}{2}A = 26.091(6) \text{ MHz.}$$

$${}^7\text{Li}, 2P_{1/2}: \Delta\nu_{2-1} = 2A = 92.047(6) \text{ MHz.}$$

The maximum deviation of the values in the table from the extrapolated values is only 8 kHz ( $1.3\sigma$ ). To the extent that different transitions are susceptible to different degrees of systematic error, this again confirms that our error estimate is reasonable.

The value of the magnetic-dipole coupling constant  $A$  in the two isotopes is compared to previous values in Table 4. Also listed is the recommended value from the review work of Arimondo, Inguscio, and Violino [2]. The result in  ${}^6\text{Li}$  is completely consistent with previous measurements, as seen from the deviation plot in Fig. 4, but the accuracy is improved by a factor of 5. In  ${}^7\text{Li}$ , our value is slightly non-overlapping with the recommended value. However, it is consistent with a recent measurement [12], which has the same accuracy as the recommended value, and an earlier less precise measurement [13]. Our accuracy is almost an order of magnitude better. The last column in the table lists the result of a recent calculation of  $A$  in  ${}^7\text{Li}$  [14], which agrees with our value at the 1.7% level.

## 5. Sodium

Sodium has one stable isotope,  ${}^{23}\text{Na}$ , with  $I = 3/2$ . Both the  $D$  lines are near 589 nm, and are accessed using a cw ring-dye laser (Coherent 699-21) operating with Rhodamine-

6G dye. Na spectroscopy is done in a 100-mm long vapor cell. The cell is heated to a temperature of 75°C and has a magnetic shield around it.

### 5.1. $D_1$ line

The hyperfine levels in the  $3P_{1/2}$  state are far apart and the individual transitions in the  $D_1$  line are well resolved. Hence we have used the standard SAS technique for spectroscopy to lock the laser and the AOM. As in the case of Li, intensity-dependent errors are checked by repeating the measurements at three laser powers. The average value of the interval is

$$^{23}\text{Na}, 3P_{1/2}: \Delta\nu_{2-1} = 2A = 188.697(14) \text{ MHz.}$$

The value of the hyperfine constant is compared to the recommended value and another published result [15] in Fig. 5. Our value is consistent with these results but the accuracy is improved by a factor of 20.

### 5.2. $D_2$ line

As mentioned earlier, the hyperfine levels in the  $3P_{3/2}$  state of  $^{23}\text{Na}$  are too close for the individual transitions in the  $D_2$  line to be resolved. Hence we have used the technique of CCS to resolve these transitions. The results of our measurements have been published previously [7]. The average values of the intervals are:

$$\begin{aligned} ^{23}\text{Na}, 3P_{3/2}: \Delta\nu_{3-2} &= 3A + B = 58.310(11) \text{ MHz,} \\ \Delta\nu_{2-1} &= 2A - B = 34.339(11) \text{ MHz.} \end{aligned}$$

In Fig. 6, we compare our values of the hyperfine constants to the recommended value and two subsequent measurements, one using time-resolved hyperfine quantum-beat spectroscopy [16] and the second using polarization quantum-beat spectroscopy [17]. Our values are consistent with the earlier values but the accuracy is improved by a factor of 5.

## 6. Potassium

Potassium has two stable isotopes:  $^{39}\text{K}$  with  $I = 3/2$  and natural abundance of 93.3%, and  $^{41}\text{K}$  with  $I = 3/2$  and natural abundance of 6.7%. The  $D_1$  line is at 770 nm and the  $D_2$  line is at 767 nm. It is difficult to obtain reliable laser diodes at these wavelengths, hence our experiments were done sometimes with a frequency-stabilized diode and sometimes with a ring-cavity Ti:sapphire laser (Coherent 899-21) similar to the ring dye laser used for the sodium experiments. Potassium spectroscopy was done in a 50-mm long vapor cell. The cell was heated to a temperature of 75°C and had a magnetic shield around it. Due to the low natural abundance of  $^{41}\text{K}$ , it is difficult to get a good absorption signal for this isotope, hence we have measured hyperfine structure only in  $^{39}\text{K}$ .

### 6.1. $D_1$ line

The hyperfine levels in the  $4P_{1/2}$  state are separated by about 58 MHz compared to the natural linewidth of 6 MHz. Thus the individual transitions in the  $D_1$  line are fairly well resolved. In a first set of experiments, we measured the interval using normal SAS to lock the laser and the AOM. Note that the crossover resonance is only 29 MHz away, which is not very far given that the experimentally obtained linewidth in SAS is around 10 MHz. The result for the interval from these measurements was 57.723(15) MHz. The slightly large error is due to the nearby crossover resonance which causes some peak pulling.

In an earlier measurement from our laboratory [18], we had measured the absolute frequencies of individual transitions in the  $D_1$  line and hence determined the hyperfine interval indirectly. The direct measurement of the interval was consistent with this earlier result. In addition, it agreed with the recommended value in Ref. [2] (from a measurement by Buck and Rabi [19] using the atomic beam magnetic resonance technique). However, there has since been a report of absolute frequency measurements on the same line using a femtosecond comb [20]. The value of the interval disagrees from our value (by  $25\sigma$  combined) and the recommended value (by  $3.5\sigma$  combined), too large to be accounted for by any known sources of error. We have therefore repeated the measurement of the interval but this time using the CCS technique. As mentioned earlier, this technique does not produce crossover resonances and the measured interval is insensitive to detuning of the control laser.

In Fig. 7, we show a typical probe transmission spectrum in  $^{39}\text{K}$  obtained with the probe locked to the  $F = 2 \rightarrow 2$  transition and the control scanning across the  $F = 2 \rightarrow 1$  transition. The scanning is done by varying the frequency of the AOM in the path of the control, so that the scan axis is properly calibrated and its linearity is guaranteed by the linearity of the voltage-controlled oscillator (vco) driving the AOM. Note that direct scanning of the laser using intracavity elements usually results in a nonlinear scan. The AOM is double passed to ensure that the direction of the control beam remains unchanged while the AOM is scanned, and the output beam intensity is stabilized by feedback control of the rf power exciting the AOM.

The open circles in the figure represent the measured spectrum while the solid curves are fits. We did two kinds of fitting to the spectrum. The first fit is to a Lorentzian lineshape with the peak center and linewidth as fit parameters. The second fit is to a density-matrix calculation of the effective three-level system taking into account the thermal velocity distribution in hot vapor, as described in our earlier work [6]. The hyperfine interval (which determines the control detuning at the peak) and the control Rabi frequency are free fit parameters. The residuals from the two fits are also shown in the figure, with the Lorentzian fit yielding slightly smaller residuals. However, the location of the peak center from both fits is the same. After fitting to several independent spectra (to take care of drifts in the vco driving the AOM), we obtain a value of 57.713(42) MHz for the interval, close to our earlier measurement and the one

by Buck and Rabi. The dashed curve shows what the spectrum would look like if the interval were 55.500 MHz as measured by Falke *et al.*

Although the spectrum obtained by scanning the AOM yields the interval, the locking technique has higher accuracy because the AOM frequency is measured while it is locked, and is not susceptible to drifts of the vco. The new result for the interval by locking the AOM is

$$^{39}\text{K}, 4P_{1/2}: \Delta\nu_{2-1} = 2A = 57.696(10) \text{ MHz},$$

which is again consistent with the above measurements and our earlier published value.

In Fig. 8, we compare this value of  $A$  with other published values. As can be seen, there are two sets of values that are in complete disagreement with each other. The recommended value and our two results are clustered on one side, while the recent result of Falke *et al.* [20] and two older measurements (which are both from the same group [21, 22]) are clustered together. The experiment of Falke *et al.* [20] has also been done with great care and takes into account many potential sources of error, hence their measurement seems to be reliable within the stated accuracy. We do not have a satisfactory explanation for such a large discrepancy.

## 6.2. $D_2$ line

As mentioned before, the hyperfine levels in the  $4P_{3/2}$  state of  $^{39}\text{K}$  are too close to be resolved completely. Hence we have used our technique of CCS to get a partially-resolved spectrum. However, the peaks are still so close that the lock point will get pulled by the nearby transition. Therefore, as described above for the  $D_1$  spectrum, we measure the intervals by scanning the AOM in the path of the control beam. The AOM is again double-passed and the output beam is intensity stabilized.

A typical probe transmission spectrum of the  $D_2$  line with the probe locked on the  $F = 2 \rightarrow F' = 3$  transition is shown in Fig. 8. We saw above in the case of the  $D_1$  line that the lineshape is described quite well by a Lorentzian curve, hence we extract the locations of the individual hyperfine transitions by doing a multipeak fit to the spectrum. As seen from the figure, the featureless residuals are less than 1% of the peak. The fit linewidth is 8.4 MHz, or only 45% larger than the natural linewidth of 5.8 MHz. After fitting to 25 spectra we obtain the average values of the intervals as

$$\begin{aligned} ^{39}\text{K}, 4P_{3/2}: \Delta\nu_{3-2} &= 3A + B = 21.107(90) \text{ MHz}, \\ \Delta\nu_{2-1} &= 2A - B = 9.280(70) \text{ MHz}. \end{aligned}$$

The slightly larger errors are due to the drift of the vco from shot to shot.

The difficulty in measuring hyperfine structure in this state is evidenced by the fact that there has only been one other measurement in recent times [20]. Our values of the hyperfine constants  $A$  and  $B$  are compared to this measurement and the recommended values in Fig. 9. The three sets are in complete agreement with each other, with our values having the smallest uncertainty. Note that the recent values in Ref. [20] are from the same work which differed so significantly for the  $D_1$  line.

## 7. Rubidium

Rubidium has two stable isotopes:  $^{85}\text{Rb}$  with  $I = 5/2$  and natural abundance of 72.2%, and  $^{87}\text{Rb}$  with  $I = 3/2$  and natural abundance of 27.8%. The  $D_1$  line at 795 nm and the  $D_2$  line at 780 nm are both accessed using frequency-stabilized diode lasers. Rb spectroscopy is done in a 50-mm long vapor cell containing both isotopes. The cell is at room temperature and has a magnetic shield around it.

### 7.1. $D_1$ line

The hyperfine levels in the  $5P_{1/2}$  state are far apart and the individual transitions in the  $D_1$  line are well resolved. Therefore we have used the standard SAS technique for spectroscopy. The results of our measurements have been published before [23], with the average values in the two isotopes as:

$$^{85}\text{Rb}, 5P_{1/2}: \Delta\nu_{3-2} = 3A = 361.936(14) \text{ MHz.}$$

$$^{87}\text{Rb}, 5P_{1/2}: \Delta\nu_{2-1} = 2A = 812.238(14) \text{ MHz.}$$

These values are compared to earlier values in Fig. 11. One of the reasons for our interest in Rb was that the values from Ref. [24] differed significantly from an earlier measurement from our laboratory [18]. In both these cases, the absolute frequencies of the individual transitions were measured and the hyperfine interval determined from their difference. By contrast, in the present work we measure the interval directly. As can be seen from the figure, the present value agrees with our earlier indirect measurement, but disagrees with the one from Ref. [24]. Note that the value for  $^{87}\text{Rb}$  from Ref. [24] also disagrees with the recommended value.

### 7.2. $D_2$ line

The hyperfine levels in the  $5P_{3/2}$  state are far apart and the individual transitions in the  $D_2$  line are well resolved. Therefore we have used the standard SAS technique for spectroscopy. As usual, we check for intensity-dependent errors by repeating the measurements at several powers. We have earlier published results in  $^{85}\text{Rb}$  using a similar technique to measure the intervals [25]. Although those results were the most accurate then, our current work improves on that precision significantly. In addition, we report results in  $^{87}\text{Rb}$  for the first time. The average values for the intervals are:

$$\begin{aligned} ^{85}\text{Rb}, 5P_{3/2}: \Delta\nu_{4-3} &= 4A + \frac{4}{5}B = 120.966(8) \text{ MHz,} \\ \Delta\nu_{3-2} &= 3A - \frac{9}{20}B = 63.424(6) \text{ MHz,} \\ \Delta\nu_{2-1} &= 2A - \frac{4}{5}B = 29.268(7) \text{ MHz.} \end{aligned}$$

$$\begin{aligned} ^{87}\text{Rb}, 5P_{3/2}: \Delta\nu_{3-2} &= 3A + B = 266.657(8) \text{ MHz,} \\ \Delta\nu_{2-1} &= 2A - B = 156.943(8) \text{ MHz,} \\ \Delta\nu_{1-0} &= A - B = 72.223(9) \text{ MHz.} \end{aligned}$$

The hyperfine constants are compared to previous values in Fig. 12. In  $^{85}\text{Rb}$ , these values are consistent with our earlier measurement and the recommended values. For  $B$ , there is a slight discrepancy from the value in Ref. [24], but this is the same work where there was a large discrepancy in the  $D_1$  line as well. For  $^{87}\text{Rb}$ , the three recent high-precision measurements are in good agreement with each other. The values in Ref. [26] have roughly the same accuracy as ours, and are obtained from absolute frequency measurements of various transitions in the  $D_2$  line. Indeed, their measurement of the  $D_2$  frequency with a precision of  $1.5 \times 10^{-11}$  has enabled us to use this line as a frequency reference along with a ring-cavity resonator for absolute optical frequency measurements of other transitions [27, 28].

## 8. Cesium

Cs has just one stable isotope,  $^{133}\text{Cs}$  with  $I = 7/2$ . The  $D_1$  line at 895 nm and the  $D_2$  line at 852 nm are both accessed using frequency-stabilized diode lasers. Cs spectroscopy is done in a 50-mm long vapor cell. The cell is at room temperature and has a magnetic shield around it.

### 8.1. $D_1$ line

The hyperfine levels in the  $6P_{1/2}$  state are more than 1 GHz apart and the individual transitions in the  $D_1$  line are well resolved. Therefore we have used the standard SAS technique to lock the laser and the AOM. The hyperfine interval is actually larger than the Doppler width, hence the spectrum has no crossover resonances. The results have been published previously [29], with the average value of the hyperfine interval as

$$^{133}\text{Cs}, 6P_{1/2}: \Delta\nu_{4-3} = 4A = 1167.654(6) \text{ MHz.}$$

Since the publication of our result, there has been a report of another high-precision measurement of the interval in this state by Gerginov *et al.* [30]. In that work, the absolute frequencies of the transitions were measured using a femtosecond frequency comb with a stated precision of 4 kHz. Our value is compared to this value and other published values in Fig. 13. Two of the previous values are also from measurements of the absolute frequencies, one using a frequency comb by Hänsch and coworkers [31], and the other from our laboratory using a Rb-stabilized ring-cavity resonator [28]. Our value is consistent with both these measurements and an earlier less precise measurement in Ref. [32], and appears inconsistent only with the most recent measurement by Gerginov *et al.* [30].

### 8.2. $D_2$ line

The hyperfine levels in the  $6P_{3/2}$  state are far apart and the individual transitions in the  $D_2$  line are well resolved. However, the measurements on the  $D_2$  line were done using our technique of CCS and not SAS. The advantages of the CCS technique for hyperfine

measurements have been highlighted earlier. In Cs, there is an additional advantage because, in normal SAS, the hyperfine peaks can get distorted and even change sign due to the effects of optical pumping and radiation pressure [33]. On the other hand, the lineshape in CCS remains symmetric even at high powers. The measurements in Cs have been published previously [6]. The large nuclear spin in  $^{133}\text{Cs}$  implies that, at sufficiently high precision, the intervals will show the effect of a small magnetic-octupole interaction (characterized by the hyperfine constant  $C$ ). The average values of the hyperfine intervals in terms of these constants are:

$$\begin{aligned} ^{133}\text{Cs}, 6P_{3/2}: \Delta\nu_{5-4} &= 5A + \frac{5}{7}B + \frac{40}{7}C = 251.037(6) \text{ MHz}, \\ \Delta\nu_{4-3} &= 4A - \frac{2}{7}B - \frac{88}{7}C = 201.266(6) \text{ MHz}, \\ \Delta\nu_{3-2} &= 3A - \frac{5}{7}B + \frac{88}{7}C = 151.232(6) \text{ MHz}. \end{aligned}$$

One of the motivations for our work on the  $6P_{3/2}$  state of Cs was that the published values of the hyperfine interval  $\Delta\nu_{5-4}$  had changed from 251.000(20) MHz in the work of Tanner and Wieman [34] to 251.092(2) MHz in the recent work of Gerginov, Derevianko, and Tanner [35], a change of 92 kHz ( $4.6\sigma$ ). This discrepancy is seen clearly in the deviation plot of the hyperfine constants in Fig. 13, comparing our values to these previous results. Our results are close to the earlier values [34], but disagree with the recent measurement by Gerginov *et al.* [35]. It is also from a measurement by Gerginov *et al.* [30] that our interval in the  $D_1$  line differs by 70 kHz.

## 9. Summary

In conclusion, we have recently developed a technique for measuring hyperfine intervals using an AOM whose frequency is directly locked to the frequency difference between two transitions. We use techniques of high-resolution laser spectroscopy to resolve hyperfine transitions in the  $D$  lines of all the alkali atoms. In lithium, we study the fluorescence signal from a collimated atomic beam excited by a laser beam at right angles. In all other atoms, we study the absorption of a probe beam through a vapor cell, in the presence of either a counter-propagating pump beam (saturated-absorption spectroscopy) or a co-propagating control beam (coherent-control spectroscopy). We are thus able to measure hyperfine intervals in the first-excited  $P_{1/2}$  and  $P_{3/2}$  states of these atoms. This yields the magnetic-dipole coupling constant  $A$  and the electric-quadrupole coupling constant  $B$  in these states. In the  $6P_{3/2}$  state of  $^{133}\text{Cs}$ , there is evidence of a small magnetic-octupole coupling constant  $C$ .

The measured hyperfine constants in the various atoms are summarized in Table 5. As discussed in earlier sections, in most cases our values are consistent with other measurements but have considerably improved precision. Improved knowledge of the hyperfine constants should prove useful to both theorists and experimentalists working with alkali atoms. The only state in which we have not measured hyperfine structure with higher precision is the  $2P_{3/2}$  state of Li, where the level spacing is smaller than the natural linewidth.

In addition, we have previously used our Rb-stabilized ring-cavity resonator to measure the absolute frequencies of the  $D$  lines in all atoms except  $^{23}\text{Na}$ . The hyperfine intervals determined from the differences in the transition frequencies match the intervals measured with the direct AOM technique, though the precision is typically five times less for the absolute-frequency method. The two techniques are very different in the way the frequencies are determined. Hence the consistency indicates that both techniques are reliable within their error bars.

Of the 17 constants listed in the Table, there are only 2 values that are discrepant from recent measurements, namely in the  $P_{1/2}$  states of  $^{39}\text{K}$  and  $^{133}\text{Cs}$ . In both cases, the recent measurements use the frequency-comb technique to measure the absolute frequencies of the transitions. However, in both cases there are other independent measurements (albeit with slightly lower precision) that agree with our results. In the case of  $^{39}\text{K}$ , there is an earlier atomic beam magnetic resonance measurement by Buck and Rabi [19], and in the case of  $^{133}\text{Cs}$ , there is a previous measurement by Hänsch and coworkers also using the frequency-comb technique [31].

Another common feature of the two frequency-comb measurements is that they use fluorescence spectroscopy from an atomic beam, while we use absorption spectroscopy in a vapor cell. Cell experiments have two advantages over the use of an atomic beam.

- (i) The line center is completely insensitive to the first-order Doppler effect. Even if there were a small misalignment angle between the pump/control and probe beams, this would result in a broadening of the line and not a shift. In a beam experiment, any deviation from perpendicularity of the atomic beam from the laser beam would result in a systematic Doppler shift.
- (ii) The cell can be magnetically shielded much better than a beam. Our residual field with the two-layer shield is 1 mG, while the residual field in beam experiments is typically 10 times larger. This could lead to correspondingly larger Zeeman shifts.

This is why we have done all our experiments with vapor cells except in the case of lithium, for which it is difficult to make vapor cells because hot lithium vapor is highly reactive and attacks most glasses.

The frequency-comb technique is known to be highly reliable. The AOM technique is also inherently free of systematic errors at this level of precision since the rf frequency can be measured with  $< 0.1$  kHz accuracy. This suggests that any discrepancy with frequency-comb measurements arises due to errors in the atomic spectrometers used, especially when the precision is being pushed to  $10^{-3}$  of the spectral linewidth. In other words, the spectral linewidth and the ability to split the line are going to limit the precision and not the measurement technique *per se*. The discrepancy in the interval for the  $6P_{1/2}$  state of  $^{133}\text{Cs}$  between our work and that of Gerginov *et al.* [30] is about 70 kHz, or 1% of the linewidth. It is conceivable that one of the two spectrometers is systematically off by this fraction of the linewidth. However, the discrepancy in the interval for the  $4P_{1/2}$  state of  $^{39}\text{K}$  from the work of Falke *et al.* [20] is 2 MHz, or 33% of the linewidth. This is too large to be accounted for by any known problems with

the spectrometer. We have also done the spectroscopy with both the SAS and the CCS techniques, and get consistent results. Further high-precision measurements with alternate techniques might shed light on these two cases.

## Acknowledgments

We thank E. Arimondo for useful discussions related to collisional shifts in hyperfine measurements. We are grateful to W. A. van Wijngaarden for help with the design of the lithium oven and to Hema Ramachandran for loan of a potassium vapor cell. This work was supported by the Department of Science and Technology and the Board of Research in Nuclear Sciences (DAE), Government of India. One of us (D.D.) acknowledges a graduate fellowship from the Council of Scientific and Industrial Research, India.

## References

- [1] M. S. Safronova, W. R. Johnson, and A. Derevianko. Relativistic many-body calculations of energy levels, hyperfine constants, electric-dipole matrix elements, and static polarizabilities for alkali-metal atoms. *Phys. Rev. A*, 60(6):4476–4487, Dec 1999.
- [2] E. Arimondo, M. Inguscio, and P. Violino. Experimental determinations of the hyperfine structures in the alkali atoms. *Rev. Mod. Phys.*, 49:31–75, 1977.
- [3] A. J. Wallard. Frequency stabilization of the helium-neon laser by saturated absorption in iodine vapour. *J. Phys. E*, 5:926–930, 1972.
- [4] W. Demtröder. *Laser Spectroscopy*. Springer-Verlag, Berlin, 1982.
- [5] A. Banerjee and V. Natarajan. Saturated-absorption spectroscopy: eliminating crossover resonances by use of copropagating beams. *Opt. Lett.*, 28:1912, 2003.
- [6] D. Das and V. Natarajan. Hyperfine spectroscopy on the  $6P_{3/2}$  state of  $^{133}\text{Cs}$  using coherent control. *Europhys. Lett.*, 72(5):740–746, 2005.
- [7] D. Das, K. Pandey, A. Wasan, and V. Natarajan. Resolving closely spaced hyperfine levels in the  $3P_{3/2}$  state of  $^{23}\text{Na}$ . *J. Phys. B*, 39:3111–3119, 2006.
- [8] R. Grimm and J. Mlynek. The effect of resonant light pressure in saturation spectroscopy. *Appl. Phys. B*, 49:179, 1989.
- [9] Conetic AA Alloy, Magnetic Shield Corporation, Perfection Mica Co., Bensenville, Illinois, USA.
- [10] F. P. D. Santos, H. Marion, S. Bize, Y. Sortais, A. Clairon, and C. Salomon. Controlling the cold collision shift in high precision atomic interferometry. *Phys. Rev. Lett.*, 89(23):233004, Nov 2002.
- [11] D. Das and V. Natarajan. Absolute frequency measurement of the lithium D lines: Precise determination of isotope shifts and fine-structure intervals. *Phys. Rev. A*, 75(5):052508, 2007.
- [12] J. Walls, R. Ashby, J. J. Clarke, B. Lu, and W. A. van Wijngaarden. Measurement of isotope shifts, fine and hyperfine structure splittings of the lithium D lines. *Eur. Phys. J. D*, 22:159–162, 2003.
- [13] G. J. Ritter. Hyperfine structure of the level of lithium-6 and lithium-7. *Can. J. Phys.*, 43:770–781, 1965.
- [14] M. Godefroid, C. F. Fischer, and P. Jönsson. Non-relativistic variational calculations of atomic properties in Li-like ions: Li I to O VI. *J. Phys. B*, 34:1079, 2001.
- [15] W. A. van Wijngaarden and J. Li. Measurement of hyperfine structure of sodium  $3P_{1/2,3/2}$  states using optical spectroscopy. *Z. Phys. D*, 32:67, 1994.
- [16] Th. Krist, P. Kuske, A. Gaupp, W. Wittmann, and H. J. Andrä. Improved  $^{23}\text{Na}$  I  $3^2P_{3/2}$  HFS measurement beyond the natural linewidth by beam laser quantum beats. *Phys. Lett.*, 61A:94–96, 1977.

- [17] Wo Yei, A. Sieradzan, and M. D. Havey. Delayed-detection measurement of atomic Na  $3p\ ^2P_{3/2}$  hyperfine structure using polarization quantum-beat spectroscopy. *Phys. Rev. A*, 48:1909–1915, 1993.
- [18] A. Banerjee, D. Das, and V. Natarajan. Absolute frequency measurements of the D<sub>1</sub> lines in  $^{39}\text{K}$ ,  $^{85}\text{Rb}$ , and  $^{87}\text{Rb}$  with  $\sim 0.1$  ppb uncertainty. *Europhys. Lett.*, 65(2):172–178, 2004.
- [19] P. Buck and I. I. Rabi. Hyperfine structure of  $\text{K}^{39}$  in the  $4P$  state. *Phys. Rev.*, 107(5):1291–1294, Sep 1957.
- [20] S. Falke, E. Tiemann, C. Lisdat, H. Schnatz, and G. Grosche. Transition frequencies of the D lines of  $^{39}\text{K}$ ,  $^{40}\text{K}$ , and  $^{41}\text{K}$  measured with a femtosecond laser frequency comb. *Phys. Rev. A*, 74(3):032503, 2006.
- [21] N. Bendali, H. T. Duong, and J. L. Vialle. High-resolution laser spectroscopy on the D<sub>1</sub> and D<sub>2</sub> lines of  $^{39,40,41}\text{K}$  using RF modulated laser light. *J. Phys. B*, 14:4231–4240, 1981.
- [22] F. Touchard, P. Guimbal, S. Büttgenbach, R. Klapisch, M. De Saint Simon, J. M. Serre, C. Thibault, H. T. Duong, P. Juncar, S. Liberman, J. Pinard, and J. L. Vialle. Isotope shifts and hyperfine structure of  $^{38-47}\text{K}$  by laser spectroscopy. *Phys. Lett.*, 108B:169–171, 1982.
- [23] D. Das and V. Natarajan. Precise measurement of hyperfine structure in the  $5^2P_{1/2}$  state of Rb. *Eur. Phys. J. D*, 37:313, 2006.
- [24] G. P. Barwood, P. Gill, and W. R. C. Rowley. Frequency measurements on optically narrowed Rb-stabilised laser diodes at 780 nm and 795 nm. *Appl. Phys. B*, 53:142–147, 1991.
- [25] U. D. Rapol, A. Krishna, and V. Natarajan. Precise measurement of the hyperfine structure in the  $5P_{3/2}$  state of  $^{85}\text{Rb}$ . *Eur. Phys. J. D*, 23:185, 2003.
- [26] J. Ye, S. Swartz, P. Jungner, and J. L. Hall. Hyperfine structure and absolute frequency of the  $^{87}\text{Rb}$   $5P_{3/2}$  state. *Opt. Lett.*, 21:1280, 1996.
- [27] A. Banerjee, D. Das, and V. Natarajan. Precise frequency measurements of atomic transitions by use of a Rb-stabilized resonator. *Opt. Lett.*, 28:1579–1581, 2003.
- [28] D. Das, A. Banerjee, S. Barthwal, and V. Natarajan. A rubidium-stabilized ring-cavity resonator for optical frequency metrology: precise measurement of the D<sub>1</sub> line in  $^{133}\text{Cs}$ . *Eur. Phys. J. D*, 38:545, 2006.
- [29] D. Das and V. Natarajan. Precise measurement of hyperfine structure in the  $6P_{1/2}$  state of  $^{133}\text{Cs}$ . *J. Phys. B*, 39:2013–2019, 2006.
- [30] V. Gerginov, K. Calkins, C. E. Tanner, J. J. McFerran, S. Diddams, A. Bartels, and L. Hollberg. Optical frequency measurements of  $6s\ ^2S_{1/2} - 6p\ ^2P_{1/2}$  (D<sub>1</sub>) transitions in  $^{133}\text{Cs}$  and their impact on the fine-structure constant. *Phys. Rev. A*, 73(3):032504, 2006.
- [31] Th. Udem, J. Reichert, R. Holzwarth, and T. W. Hänsch. Absolute optical frequency measurement of the cesium D<sub>1</sub> line with a mode-locked laser. *Phys. Rev. Lett.*, 82(18):3568–3571, May 1999.
- [32] R. J. Rafac and C. E. Tanner. Measurement of the  $^{133}\text{Cs}$   $6p\ ^2P_{1/2}$  state hyperfine structure. *Phys. Rev. A*, 56(1):1027, 1997.
- [33] O. Schmidt, K. M. Knaak, R. Wynands, and D. Meschede. Cesium saturation spectroscopy revisited: how to reverse peaks and observe narrow resonances. *Appl. Phys. B*, 59:167–178, 1994.
- [34] C. E. Tanner and C. Wieman. Precision measurement of the hyperfine structure of the  $^{133}\text{Cs}$   $6P_{3/2}$  state. *Phys. Rev. A*, 38(3):1616–1617, 1988.
- [35] V. Gerginov, A. Derevianko, and C. E. Tanner. Observation of the nuclear magnetic octupole moment of  $^{133}\text{Cs}$ . *Phys. Rev. Lett.*, 91:072501, 2003.

**Table 1.** Error budget.

Source of error	Size (kHz)
1. Statistical error	2
2. Optical pumping into Zeeman sublevels	3–5
3. Feedback loop phase shift	2
4. Collisional shifts	5

**Table 2.** Measurements of hyperfine intervals in the ground  $2S_{1/2}$  state of Li. The second column lists the transition to which the laser was locked, and the third column lists the transition to which the AOM was locked. Intensity-dependent errors were checked by repeating the measurement at three powers, as listed in columns 4 to 6.

Isotope	Laser	AOM	Interval (MHz)		
			15 $\mu$ W	28 $\mu$ W	42 $\mu$ W
$^6\text{Li}$	$\frac{3}{2} \rightarrow \frac{1}{2}$	$\frac{1}{2} \rightarrow \frac{1}{2}$	228.204	228.208	228.210
	$\frac{3}{2} \rightarrow \frac{3}{2}$	$\frac{1}{2} \rightarrow \frac{3}{2}$	228.207	228.211	228.205
$^7\text{Li}$	$2 \rightarrow 1$	$1 \rightarrow 1$	803.506	803.514	803.511
	$2 \rightarrow 2$	$1 \rightarrow 2$	803.507	803.508	803.513

**Table 3.** Measurements at different powers of hyperfine intervals in the excited  $2P_{1/2}$  state of Li.

Isotope	Laser	AOM	Interval (MHz)		
			15 $\mu$ W	28 $\mu$ W	42 $\mu$ W
$^6\text{Li}$	$\frac{3}{2} \rightarrow \frac{3}{2}$	$\frac{3}{2} \rightarrow \frac{1}{2}$	26.091	26.094	26.099
	$\frac{1}{2} \rightarrow \frac{3}{2}$	$\frac{1}{2} \rightarrow \frac{1}{2}$	26.096	26.098	26.098
$^7\text{Li}$	$2 \rightarrow 2$	$2 \rightarrow 1$	92.051	92.055	92.055
	$1 \rightarrow 2$	$1 \rightarrow 1$	92.048	92.052	92.054

**Table 4.** Comparison of results for  $A$  in the  $2P_{1/2}$  state of  $^6,7\text{Li}$  to previous values. The last column gives a theoretical calculation in  $^7\text{Li}$ .

$A$ (MHz)		Reference
$^6\text{Li}$	$^7\text{Li}$	
17.394(4)	46.024(3)	This work
17.386(31)	46.010(25)	[12]
17.48(15)	46.17(35)	[13]
17.375(18)	45.914(25)	Recommended [2]
–	45.945	Theory [14]

**Table 5.** Summary of measured hyperfine constants in the different alkali atoms. In  $^{133}\text{Cs}$ , there is evidence of a small magnetic-octupole constant  $C = 0.87(32)$  kHz. FS: fluorescence spectroscopy, SAS: saturated-absorption spectroscopy, and CCS: coherent-control spectroscopy.

Atom	State	$A$ (MHz)	$B$ (MHz)	Technique
$^6\text{Li}$	$2P_{1/2}$	17.3940(40)		Beam (FS)
$^7\text{Li}$	$2P_{1/2}$	46.0235(30)		Beam (FS)
$^{23}\text{Na}$	$3P_{1/2}$	94.3485(50)		Cell (SAS)
	$3P_{3/2}$	18.530(3)	2.721(8)	Cell (CCS)
$^{39}\text{K}$	$4P_{1/2}$	28.848(5)		Cell (CCS)
	$4P_{3/2}$	6.077(23)	2.875(55)	Cell (CCS)
$^{85}\text{Rb}$	$5P_{1/2}$	120.645(5)		Cell (SAS)
	$5P_{3/2}$	25.0403(11)	26.0084(49)	Cell (SAS)
$^{87}\text{Rb}$	$5P_{1/2}$	406.119(7)		Cell (SAS)
	$5P_{3/2}$	84.7200(16)	12.4970(35)	Cell (SAS)
$^{133}\text{Cs}$	$6P_{1/2}$	291.9135(15)		Cell (SAS)
	$6P_{3/2}$	50.28163(86)	-0.5266(57)	Cell (CCS)

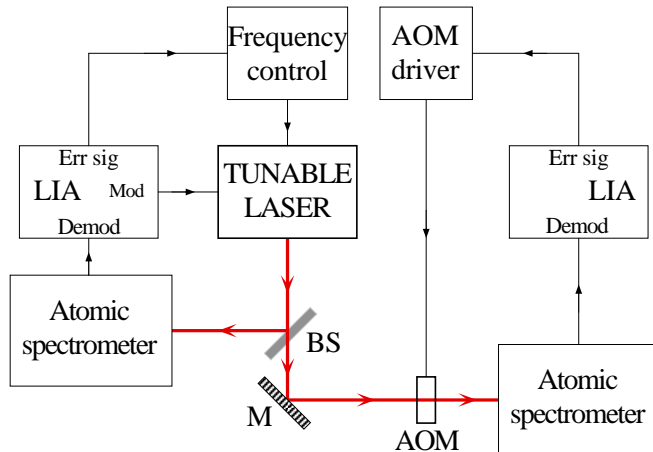


**Figure 1.** (Color online) Schematic of the experiment. Figure key – AOM: acousto-optic modulator, LIA: lock-in amplifier, BS: beam splitter, M: mirror.

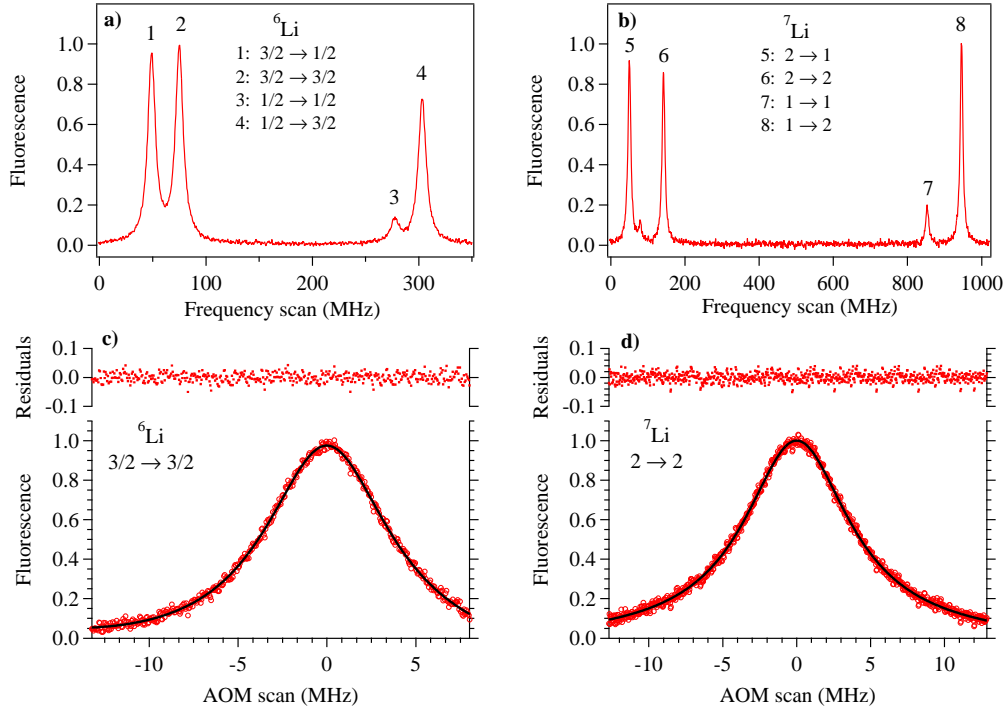


**Figure 2.** (Color online)  $D_1$  line spectra in the two isotopes of Li are shown in (a) and (b). The different hyperfine transitions are clearly resolved, and labelled as shown. There is a large increase in the gain of the PMT for (a) compared to (b) to account for the low abundance of  $^6\text{Li}$ . The small peak between peaks 5 and 6 is from the nearby  $D_2$  line in  $^6\text{Li}$ . Close-ups of peaks 2 and 6 (normalized) are shown in (c) and (d), respectively. The circles are the measured spectra and the solid lines are Lorentzian fits. The fit residuals give an idea of the signal-to-noise ratio.

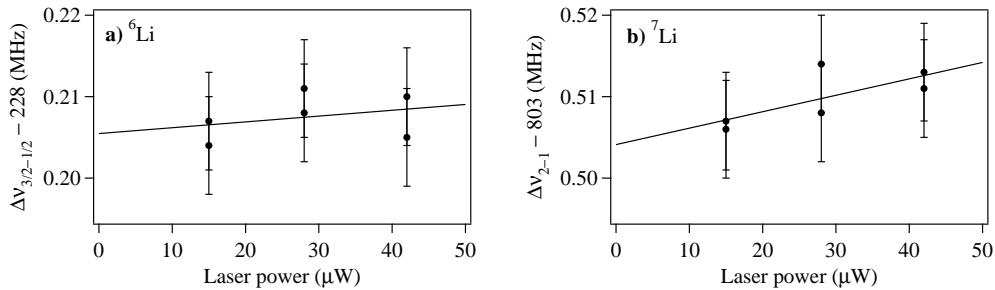


**Figure 3.** The measured hyperfine intervals in the ground state are plotted against power to check for intensity-dependent errors. The solid line is a linear fit used to extrapolate to zero power.

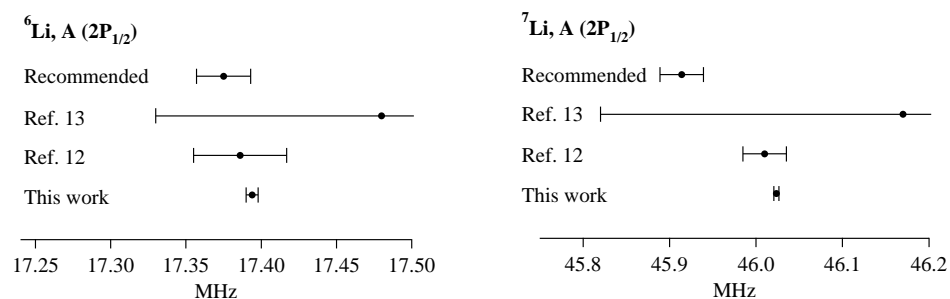


**Figure 4.** Comparison of the value of  $A$  in the  $2P_{1/2}$  state of  ${}^{6,7}\text{Li}$  obtained in this work to earlier values. Also shown is the recommended value from Ref. [2]

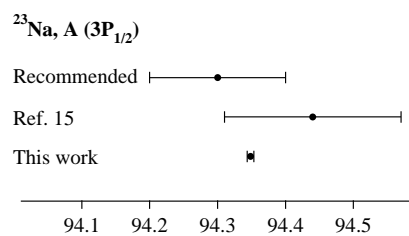


**Figure 5.** Comparison of the value of  $A$  in the  $3P_{1/2}$  state of  ${}^{23}\text{Na}$  obtained in this work to earlier values.

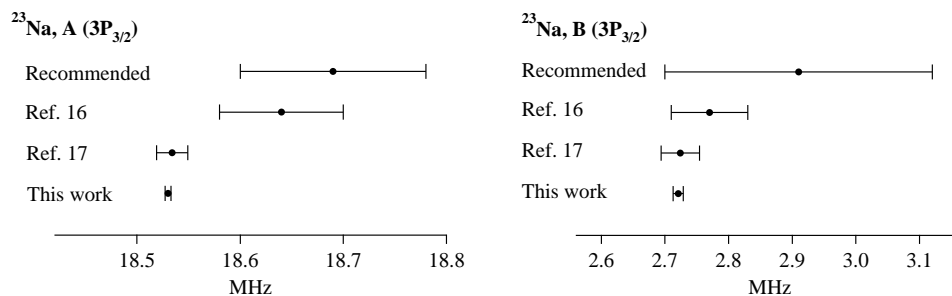


**Figure 6.** Comparison of the values of  $A$  and  $B$  in the  $3P_{3/2}$  state of  ${}^{23}\text{Na}$  obtained in this work to earlier values.

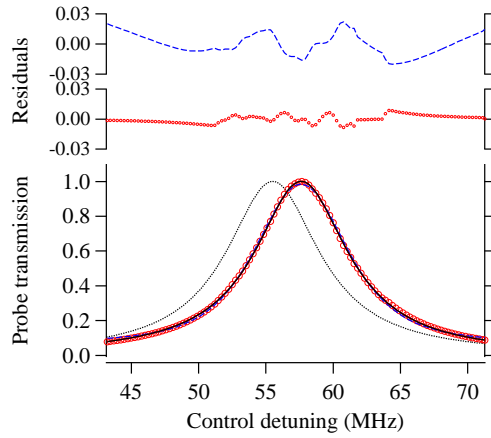


**Figure 7.** (Color online)  $D_1$  spectrum of  $^{39}\text{K}$ . The open circles show the probe transmission spectrum (normalized) using the CCS technique obtained with the probe beam locked to the  $F = 2 \rightarrow 2$  transition and the control beam scanning across the  $F = 2 \rightarrow 1$  transition. The solid curves are fits with residuals shown on top. The lower residuals are from a Lorentzian fit while the upper ones are from a density-matrix analysis. The fits yield a value of  $57.713(42)$  MHz for the interval. The dashed curve is the spectrum that would be obtained if the interval were  $55.500(84)$  MHz as measured by Falke *et al.* [20].

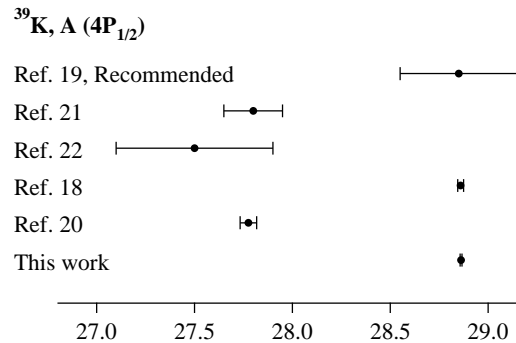


**Figure 8.** Comparison of the value of  $A$  in the  $4P_{1/2}$  state of  $^{39}\text{K}$  obtained in this work to earlier values.

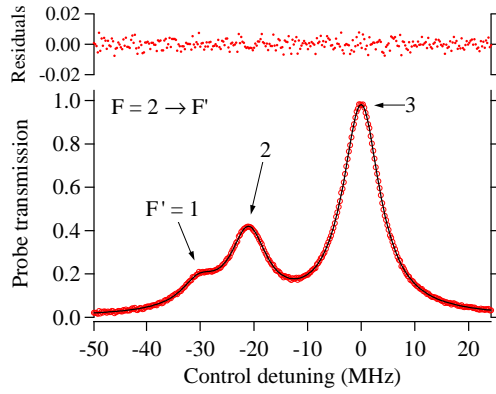


**Figure 9.** (Color online)  $D_2$  spectrum (normalized) of  $^{39}\text{K}$  without crossover resonances using the coherent-control technique. The control detuning is measured from the  $F' = 3$  peak. The open circles are the observed spectrum, while the solid curve is a three peak Lorentzian fit which yields the hyperfine intervals.

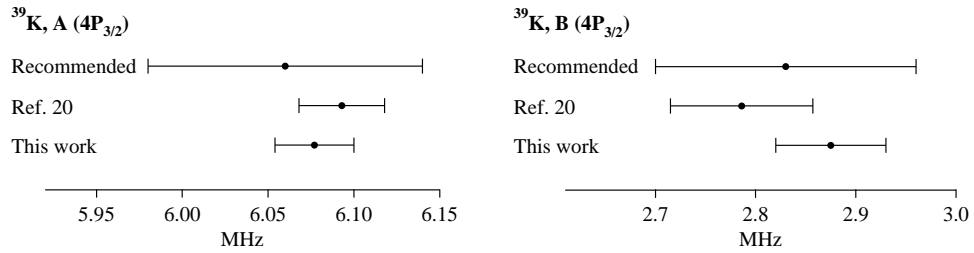


**Figure 10.** Comparison of the values of  $A$  and  $B$  in the  $4P_{3/2}$  state of  $^{39}\text{K}$  obtained in this work to earlier values.

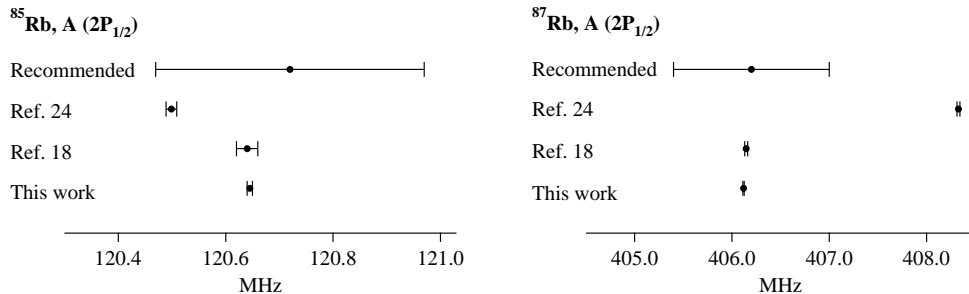


**Figure 11.** Comparison of the value of  $A$  in the  $5P_{1/2}$  state of  $^{85,87}\text{Rb}$  obtained in this work to earlier values.

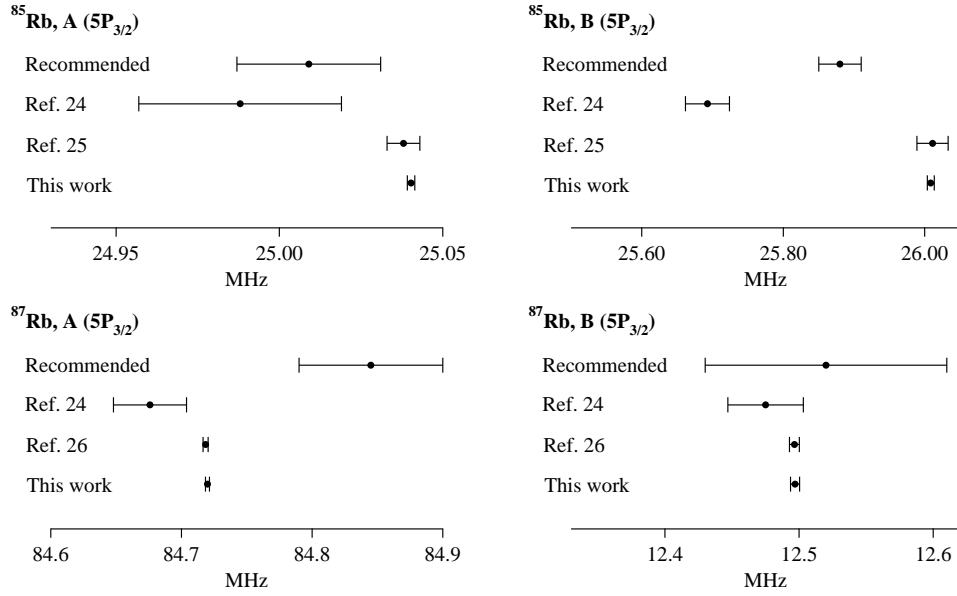


**Figure 12.** Comparison of the values of  $A$  and  $B$  in the  $5P_{3/2}$  state of  $^{85,87}\text{Rb}$  obtained in this work to earlier values.

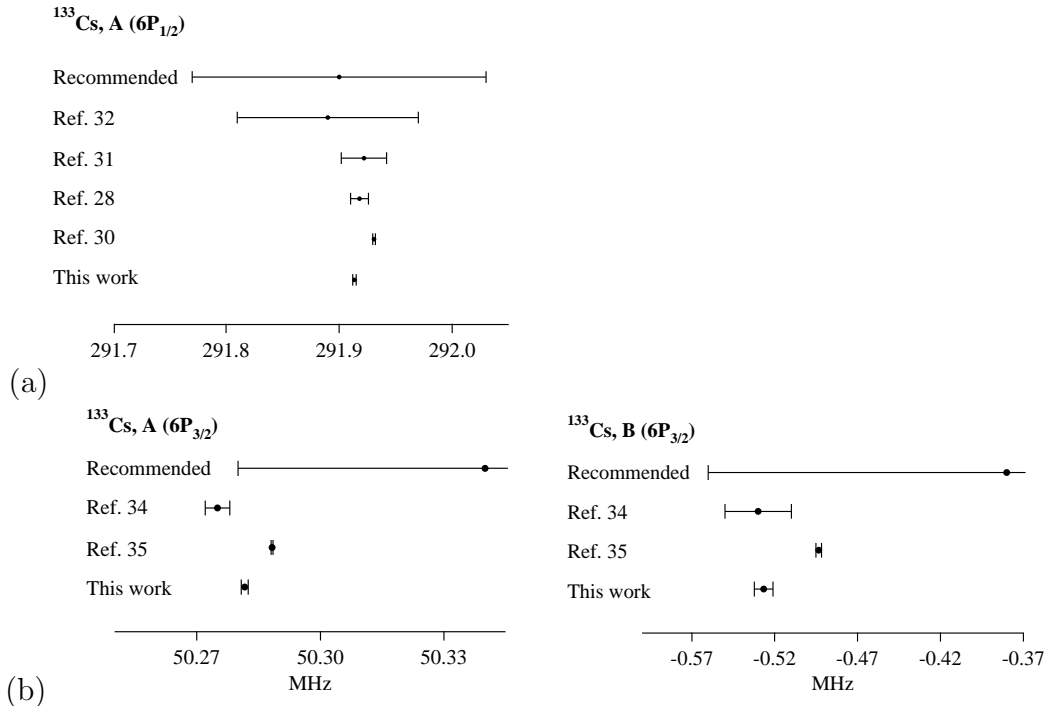


**Figure 13.** (a) Comparison of the value of  $A$  in the  $6P_{1/2}$  state of  $^{133}\text{Cs}$  obtained in this work to earlier values. (b) Comparison of the values of  $A$  and  $B$  in the  $6P_{3/2}$  state of  $^{133}\text{Cs}$  obtained in this work to earlier values.